The Journal of Clinical Pharmacology
2022, 62(1) 76–86

DOI: 10.1002/jcph.1951

Physiologically Based Pharmacokinetic Modeling to Assess the Impact of CYP2D6-Mediated Drug-Drug Interactions on Tramadol and O-Desmethyltramadol Exposures via Allosteric and Competitive Inhibition

Tao Long, PhD[1], Rodrigo Cristofoletti, PhD[1], Brian Cicali, MS[1], Veronique Michaud, BPharm, PhD[2,3], Pamela Dow, MS[2], Jacques Turgeon, BPharm, PhD[2,3], and Stephan Schmidt, BPharm, PhD, FCP[1]

Abstract

Tramadol is an opioid medication used to treat moderately severe pain. Cytochrome P450 (CYP) 2D6 inhibition could be important for tramadol, as it decreases the formation of its pharmacologically active metabolite, O-desmethyltramadol, potentially resulting in increased opioid use and misuse. The objective of this study was to evaluate the impact of allosteric and competitive CYP2D6 inhibition on tramadol and O-desmethyltramadol pharmacokinetics using quinidine and metoprolol as prototypical perpetrator drugs. A physiologically based pharmacokinetic model for tramadol and O-desmethyltramadol was developed and verified in PK-Sim version 8 and linked to respective models of quinidine and metoprolol to evaluate the impact of allosteric and competitive CYP2D6 inhibition on tramadol and O-desmethyltramadol exposure. Our results show that there is a differentiated impact of CYP2D6 inhibitors on tramadol and O-desmethyltramadol based on their mechanisms of inhibition. Following allosteric inhibition by a single dose of quinidine, the exposure of both tramadol (51% increase) and O-desmethyltramadol (52% decrease) was predicted to be significantly altered after concomitant administration of a single dose of tramadol. Following multiple-dose administration of tramadol and a single-dose or multiple-dose administration of quinidine, the inhibitory effect of quinidine was predicted to be long (≈42 hours) and to alter exposure of tramadol and O-desmethyltramadol by up to 60%, suggesting that coadministration of quinidine and tramadol should be avoided clinically. In comparison, there is no predicted significant impact of metoprolol on tramadol and O-desmethyltramadol exposure. In fact, tramadol is predicted to act as a CYP2D6 perpetrator and increase metoprolol exposure, which may necessitate the need for dose separation.

Keywords

CYP2D6-mediated drug-drug interactions, metoprolol, O-desmethyltramadol, PBPK, quinidine, tramadol

Introduction

Chronic pain is defined as pain without apparent biological value that has persisted beyond the normal healing time of 3 to 6 months.[1] It is a major public health concern, affecting 1 in 5 adults in the United States.[2] Among primary care appointments, 22% focus on chronic pain management.[3] The American College of Occupational Environmental Medicine guidelines for the chronic use of opioids[4] and the American Society of Interventional Pain Physicians[5] recommend combination medication therapy including opioids, antidepressants, nonsteroidal anti-inflammatory drugs, and anticonvulsants. The volume of opioid usage in the United States increased by up to 1177% between 1997 and 2006.[6] The most commonly used opioids in chronic pain management are oxycodone, hydrocodone, codeine, tramadol, morphine, hydromorphone, methadone, and fentanyl.

Tramadol accounts for approximately 33% of opioid use in chronic pain management.[7] It is a centrally

[1]Center for Pharmacometrics and Systems Pharmacology, Department of Pharmaceutics, College of Pharmacy, University of Florida, Orlando, Florida, USA
[2]Tabula Rasa HealthCare, Precision Pharmacotherapy Research and Development Institute, Orlando, Florida, USA
[3]Faculty of Pharmacy, Université de Montréal, Montréal, Quebec, Canada

Submitted for publication 4 May 2021; accepted 6 August 2021.

Corresponding Author:
Stephan Schmidt, BPharm, PhD, FCP, Center for Pharmacometrics and Systems Pharmacology, Department of Pharmaceutics, University of Florida, Orlando, FL 32827
Email: sschmidt@cop.ufl.edu

acting μ-opioid receptor agonist used to treat moderately severe pain. Tramadol also acts as a serotonin-norepinephrine reuptake inhibitor.[8] It is predominantly metabolized by different cytochrome P450 (CYP) enzymes to an active O-desmethyltramadol and an inactive N-desmethyltramadol metabolite.[9] The remainder is excreted unchanged in urine.[9] The biotransformation to O-desmethyltramadol is primarily mediated by CYP2D6; biotransformation to N-desmethyltramadol is mediated by CYP3A4 and CYP2B6.[9] Both O-desmethyltramadol and N-desmethyltramadol are further converted to either N,O-didesmethyltramadol or other inactive metabolites via either the same or other CYPs or by UDP-glucuronosyltransferases 1A8 and 2B7.[10] The O-desmethyltramadol metabolite is much more potent than its parent compound (≈200-300 times greater μ-opioid receptor–binding affinity).[9,11] Although tramadol per se is responsible for inhibition of the serotonin-norepinephrine reuptake that could play a role in pain perception, it is generally considered a prodrug because O-desmethyltramadol has much greater μ-opioid receptor binding affinity and has been shown to be 6 times more effective clinically.[12–14]

There is wide interindividual variability in CYP2D6 activity, due to genetic polymorphisms or phenoconversion caused by drug-drug interactions (DDIs).[9] This is expected to affect the pharmacokinetics, efficacy, and, potentially, safety of tramadol and O-desmethyltramadol. However, recent clinical studies have reported considerable amounts of O-desmethyltramadol in the plasma of CYP2D6 poor metabolizers (PMs; with no functional CYP2D6 activity) following administration of tramadol,[15–18] suggesting the involvement of other CYP enzymes in the formation of O-desmethyltramadol. Decreased CYP2D6 activity due to either allosteric inhibition or competitive inhibition could decrease formation of O-desmethyltramadol, thus compromising the overall analgesic effects and potentially increasing dosing frequency and inciting prescribing cascades in an attempt to overcome this interaction. Inhibition of CYP2D6 also increases tramadol plasma levels, which could further suppress central nervous system activity, increasing the risk for serotonergic toxicity and reducing seizure threshold.[19]

Allosteric inhibition and competitive inhibition are 2 very different types of enzyme-mediated DDIs.[20] Allosteric inhibition is a noncompetitive inhibition that involves binding of the perpetrator drug to a region of the enzyme protein structure that is spatially different from the active site where the substrate binds and is transformed. Drug binding to the allosteric site can cause conformational changes of the enzyme that render the active site no longer accessible for substrate binding or make the site unable to catalyze reactions. Almost all cases of noncompetitive inhibition are considered to be caused by allosteric regulation.[20] For this type of inhibition, the apparent Michaelis-Menten constant (K_m) remains unchanged, and the apparent maximum reaction velocity (V_{max}) decreases. Quinidine is a known allosteric inhibitor of CYP2D6.[21] In contrast, competitive inhibition involves 2 substrates competing for the same active site. Whether CYP2D6 substrates act as perpetrator or victim drugs is a function of their relative affinity for the active site as well as their concentration in the vicinity of the enzyme.[20] For this type of inhibition, the apparent K_m increases, while the apparent V_{max} remains unchanged.

Tramadol affinity for CYP2D6 is generally considered to be relatively low, while some data suggest that metoprolol would have a moderate CYP2D6 affinity.[22,23] The pattern and magnitude of interaction between 2 drugs, such as tramadol and metoprolol, depends on several factors, including the baseline bioavailability, the partial metabolic clearance through the inhibited enzymatic pathway (overall contribution of a metabolic pathway to the total clearance of the victim drug), the dose of both substrates, the sequence of administration, and the time delay between the perpetrator and victim drugs (synchronization).[24–26] Prevention of DDIs is an essential component of appropriate prescribing, as DDIs represent a major risk factor for adverse drug events in patients with several chronic diseases and polypharmacy. As a patient's pharmaceutical regimen becomes more complex, the added influence of multiple substrates competing for the same CYP450 enzyme becomes more difficult to manage.

Quantitative clinical pharmacology applications, including physiologically based pharmacokinetic (PBPK) modeling and simulation, have gained popularity for DDI assessment and are now routinely employed in drug development and regulatory evaluation. In the absence of a dedicated clinical DDI studies, PBPK models have been used to predict changes in the concentrations of victim drugs, derive dosing recommendations, and inform drug labeling. PBPK models can also help rule out the potential for a significant DDI or eliminate the need to conduct a clinical pharmacology study even when the drug candidate itself is a perpetrator.[27] This research has 2 objectives: (1) to evaluate the impact of CYP2D6-mediated DDIs via allosteric and competitive inhibitions on tramadol and O-desmethyltramadol exposure, and (2) to optimize administration times to minimize DDI risk using PBPK modeling and simulation.

Methods

Software

PBPK modeling and simulation were performed in PK-Sim version 8.0, which is part of the Open

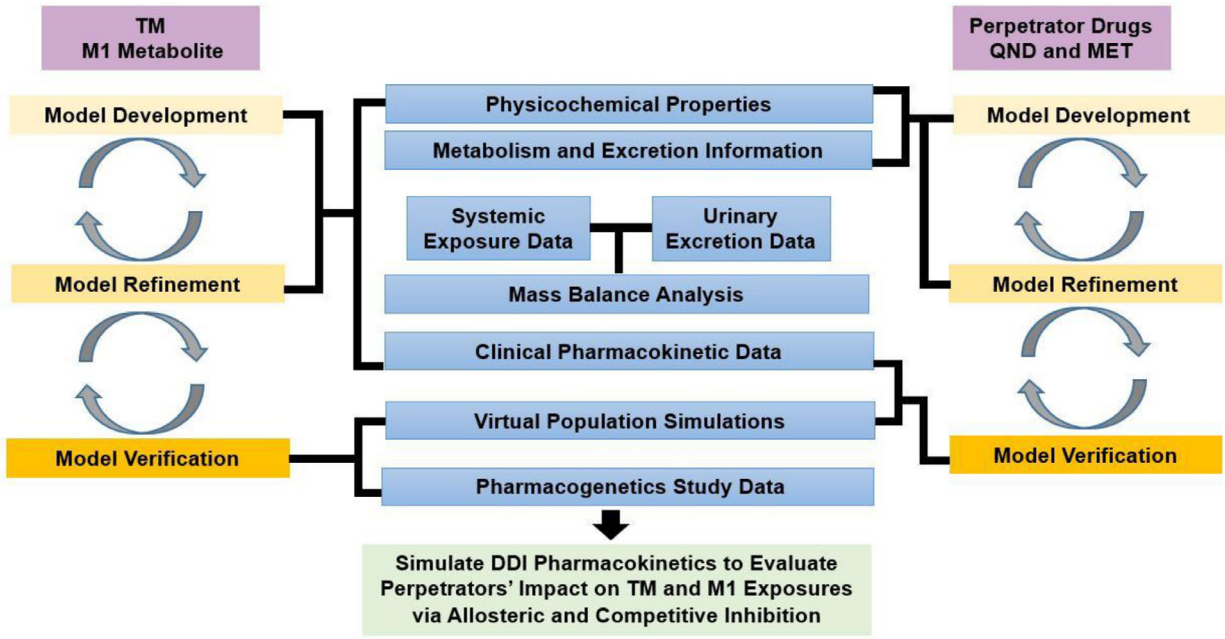

Figure 1. Schematic workflow for PBPK modeling and simulation. DDI, drug-drug interaction; MET, metoprolol; QND, quinidine; PBPK, physiologically based pharmacokinetic.

Systems Pharmacology software package (https://www.open-systems-pharmacology.org/). WebPlotDigitizer (https://automeris.io/WebPlotDigiti-zer/) was used to digitize average PK profiles from the literature.

Tramadol and O-desmethyltramadol PBPK Model Development and Verification

A summary of our PBPK modeling approach is summarized in Figure 1. Tramadol and O-desmethyltramadol disposition models were developed by integrating physicochemical drug properties (partition coefficient, ionization constant, etc) with clinical PK parameters collected from published clinical studies.[15–18,28–32] For tramadol, specific tissue-to-plasma partition coefficients were estimated using the Rodgers and Rowland method[33]; cellular permeabilities were estimated using the PK-Sim standard algorithm. Renal clearance was set to 0.13 L/h/kg, which represents ≈30% of the reported total tramadol clearance.[34,35] The remaining nonrenal clearance was considered as hepatic elimination. The unbound intrinsic hepatic clearance ($CL_{int,u}$) was derived retrogradely by integrating reported tramadol fraction unbound in plasma and the PK-Sim inputs for liver blood flow using the well-stirred liver model. The resulting $CL_{int,u}$ was further stratified to represent the relative contribution of CYP2D6 to the biotransformation of tramadol to O-desmethyltramadol.

Briefly, we derived a human mass balance diagram for tramadol and O-desmethyltramadol using urinary excretion and systemic exposure data collected from the literature.[28–32] The relative contribution of CYP2D6-mediated metabolic pathway was then translated into specific $CL_{int,u}$/CYP2D6 using intersystem extrapolation factors related to enzyme abundance and variability. The resulting tramadol fraction metabolized by CYP2D6 was further confirmed by capturing the remaining CYP2D6 activity and tramadol's pharmacokinetic (PK) profile in PMs and NMs.[15–18,36] Conceptually, to simulate the PK of tramadol and O-desmethyltramadol in PMs, the CYP2D6 metabolic pathway was completely knocked out by setting the respective $C_{lint,u} = 0$. For O-desmethyltramadol, specific tissue-to-plasma partition coefficients were estimated using the Schmitt method,[37] while cellular permeabilities were estimated using the PK-Sim standard algorithm. The renal plasma clearance of O-desmethyltramadol was set to 0.16 L/h/kg.[38]

Once developed and verified, the disposition model was expanded to account for factors impacting tramadol's oral absorption. The dissolution of tramadol immediate release formulation was modeled by a Weibull function. The dissolution time (50% dissolved) and shape was fitted to oral PK data[15] and set as 7 minutes and 0.64, which were in line with the reported dissolution profile.[39] The specific intestinal permeability was optimized based on available clinical data.[15] The overarching combined PBPK model for tramadol and O-desmethyltramadol was further verified by comparing their predicted area under the plasma concentration–time curve (AUC) ratios in CYP2D6 NMs (ie, individuals with functional CYP2D6) to

Table 1. Summary of Physicochemical and Pharmacokinetic Parameters for Tramadol and O-desmethyltramadol in the Development of the PBPK Model

Tramadol Parameters	Value	Source
Molecular weight, g/mol	263.4	[35]
logP	1.93	Optimized[a]
Solubility, mg/L	0.75 (pH = 7)	[35]
pKa	9.41 (base)	[34,35]
Fu, %	80	[34,35]
Total CL, L/h/kg	0.51 (31)[d]	[35]
In vitro intrinsic CL-CYP2D6, μL/min/pmol recombinant enzyme	0.35	Estimated[c]
In vitro intrinsic CL-CYPX, μL/min/pmol recombinant enzyme	0.03	Estimated[c]
Total hepatic CL-CYP3A4 and CYP2B6, L/h/kg	0.1	Estimated[c]
Renal CL, L/h/kg	0.13	Optimized[b]
V, L/kg	2.6-2.9	[9,35]
Elimination half-life, h	6.3 (1.4)[e]	[9,35]
t_{max}, h	1.6 (63)[d]	[35]
B:P	1.07	[34]
F	0.75	[9,35]
O-desmethyltramadol parameters	Value	Source
Molecular weight	249.3	[35]
logP	1.15	Optimized[a]
Solubility, mg/mL	3.53 (pH = 7)	[35]
pKa	9.62 (base)	[35]
f_u, %	40	Estimated
Total CL, L/h/kg	0.3	Estimated
Total hepatic CL-CYP and UGT, L/h/kg	0.27	Estimated[c]
Renal CL, L/h/kg	0.16	[38]
V, L/kg	3.2	[65]
Elimination half-life, h	7.4 (1.4)[e]	[9,35]
t_{max}, h	3.0 (51) [d]	[35]

B:P, blood to plasma concentration ratio; CL, clearance; CYP, cytochrome P450; F, bioavailability; f_u, fraction unbound in plasma; logP, partition coefficient; PBPK, physiologically based pharmacokinetic; pKa, ionization constant; t_{max}, time to maximum concentration; UGT, UDP-glucuronosyltransferase; V, volume of distribution.

[a] Optimization: In PK-Sim, it is recommended to use logMA (membrane affinity) as the input parameter. If the membrane affinity value is not available, logP can be used instead. A reasonable variation around the logP value should be allowed since this parameter is not directly related to membrane affinity.

[b] Optimization, based on reported values from T'Jollyn et al[34] and clinical observed data from Campanero et al.[52]

[c] Estimated from retrograded calculation (based on well-stirred liver model and in vitro–in vivo extrapolation).

[d] Mean (% coefficient of variation).

[e] Mean (standard deviation).

those observed in PMs, following tramadol oral administration as reported from clinical observations.[17] A summary of the final drug-specific parameters is summarized in Table 1.

Quinidine and Metoprolol PBPK Model Development and Verification

The perpetrator models were developed using both in vitro and clinical data. The parameterization input for quinidine and metoprolol PBPK models, including physiochemical (molecular weight, partition coefficient, ionization constant , etc), pharmacokinetic (volume of distribution and clearance, etc),[40–43] metabolic (V_{max} and K_m, etc),[44,45] and enzyme inhibition (quinidine-allosteric, metoprolol-competitive inhibitory constant)[46,47] parameters, are shown in Table S1-S3. The developed perpetrator models were qualified using observed clinical PK study data following administration of a single or multiple intravenous (IV) and oral dose(s) of the perpetrators (Tables S4 and S5, Figures S1 and S2[48–50]).

DDI Simulations for Allosteric and Competitive CYP2D6 Inhibition

Once independently developed and verified, PBPK models for tramadol/O-desmethyltramadol and quinidine or metoprolol were combined in simulations to evaluate the impact of allosteric (quinidine) and competitive (metoprolol) inhibition on tramadol and O-desmethyltramadol PK. To this end, we evaluated different scenarios that are relevant for drug development and regulatory evaluation as well as clinical practice.

For allosteric CYP2D6 inhibition via quinidine, we evaluated 3 main scenarios. In scenario 1, a single oral dose of quinidine (400 mg) was given concomitantly with a single oral dose of tramadol (100 mg) in accordance with the current FDA Clinical Drug Interaction Studies Guidance for short half-life drugs (≈6 hours for tramadol) showing time-independent PK.[51] In scenario 2, tramadol (100 mg, 4 times daily) was dosed to steady state before concomitant administration of a single oral dose of quinidine (400 mg) at 30 hours (T0). Both of the PK metrics AUC over the dosing interval (eg, $AUC_{0\text{-}6}$, $AUC_{6\text{-}12}$, etc.) and AUC from the last dose to infinity (eg, $AUC_{0\text{-}\infty}$, $AUC_{6\text{-}\infty}$, etc.) were evaluated and their respective AUC ratios (AUCR) were calculated. In scenario 3, tramadol (100 mg 4 times daily) and quinidine (400 mg 4 times daily) were concomitantly administered and both dosed to steady state to order to account for interactions scenarios encountered in the clinic.

For the competitive CYP2D6 inhibition via metoprolol, a single oral dose of metoprolol tartrate (100 mg, immediate-release [IR]) was administered concomitantly with a single 100-mg oral dose of tramadol. We also evaluated delayed metoprolol administration regimens (ie, delayed by 2 and 4 hours) to determine if the interaction between metoprolol and tramadol could be overcome by dose separation. Finally, we evaluated the impact of tramadol on metoprolol pharmacokinetics, as results from a recent in vitro study suggest that tramadol has a higher affinity for CYP2D6 than metoprolol,[45] that is, that tramadol may act as the perpetrator rather than the victim drug.

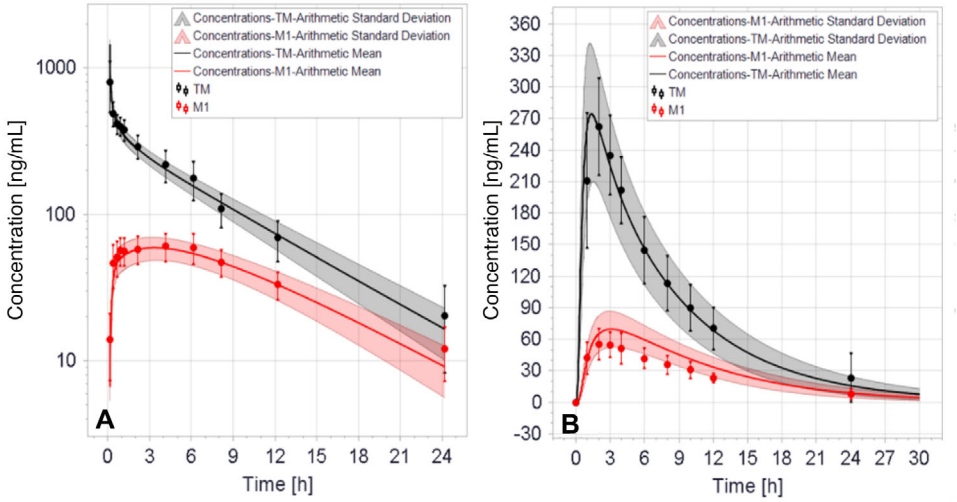

Figure 2. Observed vs predicted tramadol (TM; in black) and O-desmethyltramadol (M1; in red) concentration-time profiles following administration of (A) 100-mg intravenous infusion of tramadol over 10 minutes and (B) 100-mg tramadol, immediate-release tablet, administered orally. Shaded area represents predicted mean ± standard deviation.

All simulations were carried out in a virtual population consisting of 100 healthy White subjects aged between 25 and 55 years (1:1 ratio of men to women), which were all CYP2D6 NMs. Individual demographics, such as weight, BMI, and organ volumes, among others, were estimated from the built-in expression database available within the PK-Sim software.

Results

PBPK Model Development and Verification

Tramadol and O-desmethyltramadol disposition pathways and their relative contributions are shown in Figure S3. Approximately 26% of the administered dose of tramadol is excreted unchanged in urine. Fifty-three per cent of a tramadol dose is transformed to O-desmethyltramadol (mainly by CYP2D6, 38% of the administered dose), while CYP3A4 and CYP2B6 contribute 21% to its metabolic clearance leading to the formation of N-desmethyltramadol, suggesting that CYP2D6 accounts for ≈51% of tramadol's hepatic clearance. For O-desmethyltramadol, 38% is excreted unchanged in urine, while 63% undergoes further transformation by phase 1 and 2 metabolism.

Visual inspection of the plasma concentration-time curves overlapping predicted and observed PK profiles for tramadol and O-desmethyltramadol after IV and oral administration of tramadol confirms that model predictions capture the central tendency and variability in tramadol and O-desmethyltramadol systemic exposure in healthy adults (Figure 2).[15,52] Model adequacy was also confirmed quantitatively as the ratios between observed and predicted PK metrics were within a 1.25-fold range (Table 2). Furthermore, the predictive performance of the model was assessed by an external model verification, where model-based predictions were compared to clinical data in NMs and PMs that were not used during model development (Table 3). The predicted PM/NM exposure ratios were 1.52 and 0.44 for tramadol and O-desmethyltramadol, respectively, which are consistent with observed ratios of 1.44 and 0.37 in clinical studies.[17]

DDI Simulations for Allosteric and Competitive CYP2D6 Inhibition

Concomitant single-dose administration of tramadol and quinidine (scenario 1) increases tramadol $AUC_{0\text{-}\infty}$ by 51% and decreases O-desmethyltramadol $AUC_{0\text{-}\infty}$ by 52%. Under conditions of a single tramadol dose administration, delaying quinidine administration by 4 hours attenuated the magnitude of the predicted DDI, resulting in a 21% rather than a 51% increase in tramadol AUC and a 21% rather than 52% decrease in O-desmethyltramadol AUC. AUCRs are shown in Table 4. In scenario 2, CYP2D6 inhibition associated with a single dose of quinidine leads time-dependent changes in tramadol and O-desmethyltramadol mean plasma concentrations: we observed a 16% to 41% increase in the steady-state tramadol ($AUC_{\tau,ss}$) and a 9% to 51% decrease in the O-desmethyltramadol $AUC_{\tau,ss}$ within 48 hours after quinidine administration. The magnitude of changes in tramadol and O-desmethyltramadol exposure first increases and then gradually decreases, with the maximum exposure changes taking place at approximately 12 to 18 hours after quinidine administration (Table 4). CYP2D6 inhibition following a single dose of quinidine was predicted to last ≈42 hours, at which point both tramadol and O-

Table 2. Observed (OBS) Versus Predicted (PRED) Pharmacokinetic Parameters of Tramadol and O-desmethyltramadol Following Administration of a Single Dose of 100 mg Tramadol Via Intravenous Infusion (10 Minutes) or Oral Administration

	C_{max}, (ng/mL)—Tramadol			$AUC_{0-\infty}$ (mg • h/L)—Tramadol			C_{max} (ng/mL)—O-desmethyltramadol			$AUC_{0-\infty}$ (mg • h/L)—O-desmethyltramadol		
Route of Administration	OBS	PRED	OBS/PRED	OBS	PRED	OBS/PRED	OBS	PRED	OBS/PRED	OBS	PRED	OBS/PRED
Intravenous infusion [52]	807 (304)	1436 (119)	0.56	3.16 (0.62)	3.01 (0.45)	1.05	61 (13)	57 (10)	1.07	1.02 (0.17)	0.85 (0.17)	1.20
Oral administration [15]	273 (46)	300 (71)	0.91	2.60 (0.44)	2.50 (0.66)	1.04	59 (14)	71 (17)	0.83	0.75 (0.12)	0.91 (0.23)	0.82

$AUC_{0-\infty}$, area under the plasma concentration–time curve from time 0 to infinity; C_{max}, maximum concentration.
Mean (SD) for C_{max} and $AUC_{0-\infty}$.

desmethyltramadol steady-state exposure changes fell below 20% (Table 4). In scenario 3, $AUCR_{\tau,ss}$ for tramadol and O-desmethyltramadol were 1.57 and 0.4, respectively, indicating maximum inhibition of CYP2D6-mediated biotransformation of tramadol into O-desmethyltramadol by quinidine (Table 4).

In comparison, our simulations showed no impact of metoprolol on the systemic exposure of tramadol and O-desmethyltramadol, with $AUCR_{0-\infty}$ being 1.01. However, tramadol was predicted to increase metoprolol exposure by ≈50% as shown in Table 5. The magnitude of this DDI could be significantly mitigated by dose separation. For example, delaying the tramadol administration by 2 hours, reduced the predicted increase in metoprolol exposure to <20% (Table 5).

Discussion

In this study, we developed and verified a combined PBPK model for tramadol and O-desmethyltramadol in a stepwise fashion. First, we determined the relative contribution of hepatic and renal clearance pathways to the elimination of tramadol and O-desmethyltramadol. Furthermore, we reproduced the individual contribution of different metabolic enzymes to the biotransformation of tramadol into O-desmethyltramadol. The results of this analysis suggest that CYP2D6 accounts for ≈51% of tramadol's hepatic clearance, which is in line with values reported in literature (43%-48%).[53–56] The results further suggest that ≈20% of tramadol's hepatic biotransformation to O-desmethyltramadol is mediated by an unidentified CYP450 isoform, which could explain noticeable amounts of O-desmethyltramadol reported for CYP2D6 PMs.[15–18] The combined PBPK model for tramadol and O-desmethyltramadol was developed and externally verified. Overall, our combined PBPK model for tramadol and O-desmethyltramadol was able to reproduce clinical observations well, with the exception of tramadol maximum concentration following a 10-minute IV infusion, which was slightly underpredicted. This underprediction could be explained by the sparse and variable sampling around maximum concentration in the clinical data used for model verification.

In addition to the combined PBPK model for tramadol and O-desmethyltramadol, we developed and verified separate models for quinidine and metoprolol. These models were able to reproduce well clinical observations for both quinidine and metoprolol following single- and multiple-dose administration (ratios of predicted and observed PK metrics were within 1.25 range).[41,49,50] Once developed and verified, victim and perpetrator models were combined to predict the impact of allosteric (quinidine) and competitive

Table 3. Observed (OBS) Versus Predicted (PRED) $AUC_{0-\infty}$ of Tramadol and O-desmethyltramadol in CYP2D6 Poor Metabolizers (PMs) Versus CYP2D6 Normal Metabolizers (NMs)

	Group	$AUC_{0-\infty}$—Tramadol, mg • h/L	AUCR[a] Tramadol	fm[a], %	$AUC_{0-\infty}$—O-desmethyltramadol, mg • h/L	AUCR[a]—O-desmethyltramadol
OBS[17]	PM	3.14	1.44	31	0.35	0.37
	NM	2.18			0.95	
PRED	PM	3.80	1.52	34	0.4	0.44
	NM	2.50			0.9	

$AUC_{0-\infty}$, area under the plasma concentration–time curve from time 0 to infinity; fm, fraction metabolized.
For PMs, their CYP2D6 intrinsic clearance was set to zero in model prediction.
[a] $AUCR = AUC(PM)/AUC(EM) = 1/(1 - fm)$.

Table 4. AUCR for Tramadol and O-desmethyltramadol

Scenario 1: $AUC_{0-\infty}$	Tramadol AUCR	O-desmethyltramadol AUCR
w/, concomitant administration	1.51	0.48
w/, delayed administration of quinidine by 4 h	1.21	0.79
w/, delayed administration of quinidine by 8 h	1.12	0.89
Scenario 2: AUC_{τ}	**Tramadol AUCR**	**O-desmethyltramadol AUCR**
AUC_{0-6h}	1.29	0.71
AUC_{6-12h}	1.35	0.49
AUC_{12-18h}	1.41	0.49
AUC_{18-24h}	1.40	0.56
AUC_{24-30h}	1.36	0.65
AUC_{30-36h}	1.31	0.74
AUC_{36-42h}	1.25	0.82
AUC_{42-48h}	1.16	0.91
Scenario 2: $AUC_{last\ dose-\infty}$	**Tramadol AUCR**	**O-desmethyltramadol AUCR**
$AUC_{0h-\infty}$	1.43	0.66
$AUC_{6h-\infty}$	1.59	0.67
$AUC_{12h-\infty}$	1.57	0.73
$AUC_{18h-\infty}$	1.61	0.90
$AUC_{24h-\infty}$	1.52	0.84
$AUC_{30h-\infty}$	1.42	0.86
$AUC_{36h-\infty}$	1.33	0.92
$AUC_{42h-\infty}$	1.25	0.97
Scenario 3: $AUC_{\tau-ss}$	**Tramadol-AUCR**	**O-desmethyltramadol-AUCR**
	1.57	0.40

AUC, area under the plasma concentration–time curve; $AUC_{0-\infty}$, area under the plasma concentration–time curve from time 0 to infinity; $AUC_{\tau-ss}$, area under the plasma concentration–time curve over the dosing interval at steady state; AUCR, area under the plasma concentration–time curve ratio.
AUCR, AUC with (w/) quinidine/AUC without quinidine. Scenario 1: tramadol (100 mg, single dose) and quinidine (400 mg, single dose) were concomitantly or delayed administered. Scenario 2: tramadol (100 mg 4 times daily) was dosed to steady state with coadministration of quinidine (400 mg single dose) at 30 h. T0 = 30 h. Scenario 3: tramadol (100 mg 4 times daily) and quinidine (400 mg 4 times daily) were concomitantly administered to steady state.

Table 5. Metoprolol $AUC_{0-\infty}$ With Versus $AUC_{0-\infty}$ Without Concomitant or Delayed Administration of a Single Dose of Tramadol (100 mg)

Tramadol Administration	Metoprolol $AUC_{0-\infty}$, mg • h/L	AUCR
w/o	0.50 (0.36-0.74)	
w/, concomitant administration	0.74 (0.52-1.19)	1.48
w/, delayed administration of tramadol by 2 h	0.59 (0.42-0.89)	1.18
w/, delayed administration of tramadol by 4 h	0.55 (0.39-0.83)	1.10

$AUC_{0-\infty}$, area under the plasma concentration–time curve from time 0 to infinity; AUCR, area under the plasma concentration–time curve ratio.
Median (90% prediction interval). AUCR, AUC with (w/) tramadol/AUC without (w/o) tramadol.

(metoprolol) CYP2D6 inhibition on tramadol and O-desmethyltramadol exposure under various conditions.

For the allosteric CYP2D6 inhibition by quinidine, we evaluated 3 scenarios. In the first scenario, we followed the current FDA Guidance for Industry on Clinical Drug Interaction Studies—Cytochrome P450 Enzyme- and Transporter-Mediated Drug Interactions.[51] According to the guidance, an inhibitor can be administered as a single dose if (1) single and multiple doses of the inhibitor are expected to have similar effects on the enzyme of interest and (2) inhibition is not time dependent. In addition, a single dose of the substrate is acceptable if the substrate does not show time-dependent PK (eg, autoinhibition or autoinduction). Since both quinidine and tramadol meet the above-mentioned criteria, we considered concomitant or delayed administrations of single oral doses of quinidine and tramadol in our scenario 1. Results indicate that there is a significant interaction between quinidine and tramadol, which could be attenuated by dose separation (administration of quinidine after the single dose of tramadol). However, this strategy is not of clinical relevance as tramadol requires repeated administration during the day, and CYP2D6 inhibition by quinidine requires about 4 to 5 quinidine half-lives to wear off.

In the second scenario, we accounted for the need of repeated tramadol dosing for chronic pain management. Therefore, tramadol was given orally 4 times daily and dosed to steady state before a single oral dose of quinidine was given. Our results show that CYP2D6 inhibition was most pronounced between 12 and 18 hours after quinidine administration (41% increase in tramadol $AUC_{\tau,ss.}$ and 51% decrease in O-desmethyltramadol $AUC_{\tau,ss.}$) and wore off as quinidine concentrations decreased. Similar results were observed when both tramadol and quinidine were concomitantly administered to steady state (scenario 3). The simulations also showed that CYP2D6 allosteric inhibition by quinidine appears to be long lasting (about 42 hours). Therefore, it cannot be overcome clinically by dose separation as shown in scenarios 2 and 3. This finding is consistent with a previous review paper showing that dose separation will not alleviate allosteric inhibition.[20] Given the significant CYP2D6 inhibition and the 4-times-daily dosing regimens of both drugs, coadministration of quinidine and tramadol should be avoided clinically.

For the competitive inhibition with metoprolol, our results indicate that concomitant administration of metoprolol did not significantly affect the exposure of tramadol and O-desmethyltramadol. This was somewhat surprising, as previous drug interaction studies between metoprolol and CYP2D6 low-affinity substrates had suggested that metoprolol was a moderate affinity substrate that could act as a perpetrator drug.[22,23] In contrast, recent in vitro characterization of CYP2D6 substrate affinities suggested that tramadol has greater affinity than metoprolol for CYP2D6.[45] Hence, our simulations indicate that tramadol acts as perpetrator and will increase total metoprolol exposure ($AUC_{0-\infty}$) by approximately 48%.

Metoprolol is a second-generation β-blocker with high selectivity for $\beta 1$ adrenoceptors. $\beta 1$ selectivity for metoprolol diminishes once plasma concentrations exceed 300 nmol/L resulting in inhibition of $\beta 2$ adrenoceptors in the bronchial and vascular musculature.[57] Our simulations show that following competitive CYP2D6 inhibition via tramadol, metoprolol peak plasma concentrations were elevated to 120 ng/mL ($\approx$450 nmol/L) following repeated administration of 100 mg of metoprolol, which is sufficient to exceed the reported $\beta 1$ selectivity threshold.[57] It may consequently be worthwhile exploring clinical outcomes data to determine if adverse events associated with $\beta 2$ adrenoceptor blockage, such as bronchoconstriction, bronchospasm, and vasoconstriction, actually occur clinically. At the same time, our simulation results indicate that delayed administration of tramadol by 2 hours significantly reduces the interaction with metoprolol resulting in a <20% increase in metoprolol $AUC_{0-\infty}$.

It has further been suggested that the SLC22A1 organic cation transporter (OCT1) plays an important role in the disposition of tramadol active metabolite O-desmethyltramadol. For example, the polymorphic OCT1 has been shown to play an additional role in O-desmethyltramadol exposure in neonates, suggesting that OCT1 is already active early after birth, which may impact the disposition of other OCT1 substrates in this population.[58] Furthermore, loss-of-function polymorphisms in OCT1 have been associated with reduced postoperative tramadol consumption, but the respective mechanism is not completely understood yet.[59]

The expression of OCT1 at the blood-brain barrier (BBB) is also the subject of ongoing investigation, and resultant data can be used to further refine our PBPK model as well as our understanding of observed variability in clinical response to tramadol as it becomes available. It is also widely accepted that opioid-mediated pain relief and euphoria depends on the ability of opioids to cross the BBB. Previous studies in animals have shown that tramadol rapidly penetrates the BBB.[60,61] Similar results were obtained with human immortalized brain capillary endothelial cells.[61] The situation is somewhat more complex for perpetrators. While the moderately lipophilic metoprolol is readily able to cross the BBB,[62] quinidine has restricted access to the brain due to the ABCB1-mediated active efflux at the BBB.[63] This difference in the perpetrators' ability to cross the BBB becomes important as CYP2D6 is also expressed to various degrees in the brain.[64] However, the relative contribution of local O-desmethyltramadol formation in the brain to tramadol overall efficacy and safety profile is currently not yet fully understood and warrants further investigation.

Conclusions

There is a differentiated impact of quinidine and metoprolol via CYP2D6 inhibition on tramadol and O-desmethyltramadol pharmacokinetics. Following allosteric inhibition by single dose of quinidine, exposure of tramadol was increased and exposure of O-desmethyltramadol was decreased. This DDI cannot be overcome clinically when repeated 4-times-daily tramadol dosing is used. In comparison, there is no significant impact of metoprolol on tramadol and O-desmethyltramadol exposure. To the contrary, we found that tramadol acts as a CYP2D6 perpetrator and increases the exposure of metoprolol, which may be mitigated by dose separation. To better understand the impact of these DDIs on drug efficacy and safety, linking the developed PBPK models to representative

pharmacodynamic end-point models consequently provides a logical next step for this research.

Acknowledgments

The authors acknowledge Dr. Karel Allegaert for providing his expert advice, insightful comments, and critical discussion of the results of this research project.

Conflicts of Interest

V.M., P.D., and J.T. are employees and shareholders of Tabula Rasa HealthCare. The other authors declare no conflicts of interest.

Funding

Tabula Rasa HealthCare funded this research.

Data Sharing Statement

The data supporting the findings of this study may be shared on request from the corresponding author Dr. Stephan Schmidt at sschmidt@cop.ufl.edu .

References

1. Trescot AM, Boswell MV, Atluri SL, et al. Opioid guidelines in the management of chronic non-cancer pain. *Pain Physician*. 2006;9(1):1-39.
2. Zelaya CE, Dahlhamer JM, Lucas JW, Connor EM. *Chronic Pain and High-Impact Chronic Pain Among U.S. Adults, 2019*. Hyattsville, MD: National Center for Health Statistics; 2020. NCHS Data Brief 390.
3. Rasu RS, Vouthy K, Crowl AN, et al. Cost of pain medication to treat adult patients with nonmalignant chronic pain in the United States. *J Manag Care Spec Pharm*. 2014;20(9):921-928.
4. Hegmann KT, Weiss MS, Bowden K, et al. ACOEM practice guidelines: opioids for treatment of acute, subacute, chronic, and postoperative pain. *J Occup Environ Med*. 2014;56(12):e143-e159. https://doi.org/10.1097/JOM.0000000000000352.
5. Manchikanti LAS, Atluri S, Balog CC, et al. American Society of Interventional Pain Physicians (ASIPP) guidelines for responsible opioid prescribing in chronic non-cancer pain: part 2–guidance. *Pain physician*. 2012.
6. Manchikanti LAS. Therapeutic opioids: a ten-year perspective on the complexities and complications of the escalating use, abuse, and nonmedical use of opioids. *Pain Physician*. 2008.
7. Mordecai L, Reynolds C, Donaldson LJ, de CWAC. Patterns of regional variation of opioid prescribing in primary care in England: a retrospective observational study. *Br J Gen Pract*. 2018;68(668):e225-e233.
8. Leppert W. Tramadol as an analgesic for mild to moderate cancer pain. *Pharmacol Rep*. 2009;61(6):978-992.
9. Grond S, Sablotzki A. Clinical pharmacology of tramadol. *Clin Pharmacokinet*. 2004;43(13):879-923.
10. Lehtonen P, Sten T, Aitio O, et al. Glucuronidation of racemic O-desmethyltramadol, the active metabolite of tramadol. *Eur J Pharm Sci*. 2010;41(3-4):523-530.
11. Raffa RB, Buschmann H, Christoph T, et al. Mechanistic and functional differentiation of tapentadol and tramadol. *Expert Opin Pharmacother*. 2012;13(10):1437-1449.
12. Grond S, Sablotzki A. Clinical pharmacology of tramadol. *Clin Pharmacokinet*. 2004;43:879-923. https://doi.org/10.2165/00003088-200443130-00004.
13. Leppert W. CYP2D6 in the metabolism of opioids for mild to moderate pain. *Pharmacology*. 2011;87(5-6):274-285.
14. Samer CF, Lorenzini KI, Rollason V, Daali Y, Desmeules JA. Applications of CYP450 testing in the clinical setting. *Mol Diagn Ther*. 2013;17(3):165-184.
15. Fliegert F, Kurth B, Gohler K. The effects of tramadol on static and dynamic pupillometry in healthy subjects–the relationship between pharmacodynamics, pharmacokinetics and CYP2D6 metaboliser status. *Eur J Clin Pharmacol*. 2005;61(4):257-266.
16. Garcia-Quetglas E, Azanza JR, Sadaba B, Munoz MJ, Gil I, Campanero MA. Pharmacokinetics of tramadol enantiomers and their respective phase I metabolites in relation to CYP2D6 phenotype. *Pharmacol Res*. 2007;55(2):122-130.
17. Pedersen RS, Damkier P, Brosen K. Enantioselective pharmacokinetics of tramadol in CYP2D6 extensive and poor metabolizers. *Eur J Clin Pharmacol*. 2006;62(7):513-521.
18. Kirchheiner J, Keulen JT, Bauer S, Roots I, Brockmoller J. Effects of the CYP2D6 gene duplication on the pharmacokinetics and pharmacodynamics of tramadol. *J Clin Psychopharmacol*. 2008;28(1):78-83.
19. Beakley BD, Kaye AM, Kaye AD. Tramadol pharmacology side effects and serotonin syndrome: a review. *Pain Physician*. 2015;18(4):395-400.
20. Deodhar M, Al Rihani SB, Arwood MJ, et al. Mechanisms of CYP450 inhibition: understanding drug-drug interactions due to mechanism-based inhibition in clinical practice. *Pharmaceutics*. 2020;12(9):846.
21. McLaughlin LA, Paine MJ, Kemp CA, et al. Why is quinidine an inhibitor of cytochrome P450 2D6? The role of key active-site residues in quinidine binding. *J Biol Chem*. 2005;280(46):38617-38624.
22. Bain KT, Knowlton CH. Role of opioid-involved drug interactions in chronic pain management. *J Osteop Med*. 2019;119(12):839-847.
23. Shu-Feng Z, Jun-Ping L, Xin-Sheng L. Substrate specificity, inhibitors and regulation of human cytochrome P450 2D6 and implications in drug development. *Curr Med Chem*. 2009;16(21):2661-2805.
24. Zakrzewski-Jakubiak H, Doan J, Lamoureux P, Singh D, Turgeon J, Tannenbaum C. Detection and prevention of drug-drug interactions in the hospitalized elderly: utility of new cytochrome P450-based software. *Am J Geriatr Pharmacother*. 2011;9(6):461-470.
25. Turgeon J, Michaud V. Clinical decision support systems: great promises for better management of patients' drug therapy. *Expert Opin Drug Metab Toxicol*. 2016;12(9):993-995.
26. Doan J, Zakrzewski-Jakubiak H, Roy J, Turgeon J, Tannenbaum C. Prevalence and risk of potential cytochrome P450-mediated drug-drug interactions in older hospitalized patients with polypharmacy. *Ann Pharmacother*. 2013;47(3):324-332.
27. Zhao P, Zhang L, Grillo JA, et al. Applications of physiologically based pharmacokinetic (PBPK) modeling and simulation during regulatory review. *Clin Pharmacol Ther*. 2011;89(2):259-267.
28. Ardakani YH, Rouini MR. Pharmacokinetics of tramadol and its three main metabolites in healthy male and female volunteers. *Biopharm Drug Dispos*. 2007;28(9):527-534.
29. Overbeck P, Blaschke G. Direct determination of tramadol glucuronides in human urine by high-performance liquid chromatography with fluorescence detection. *J Chromatogr B Biomed Sci Appl*. 1999;732(1):185-192.

30. Paar WD, Poche S, Gerloff J, Dengler HJ. Polymorphic CYP2D6 mediates O-demethylation of the opioid analgesic tramadol. *Eur J Clin Pharmacol*. 1997;53(3-4):235-239.
31. Rudaz S, Veuthey JL, Desiderio C, Fanali S. Simultaneous stereoselective analysis by capillary electrophoresis of tramadol enantiomers and their main phase I metabolites in urine. *J Chromatogr A*. 1999;846(1-2):227-237.
32. Soetebeer UB, Schierenberg MO, Schulz H, Andresen P, Blaschke G. Direct chiral assay of tramadol and detection of the phase II metabolite O-demethyl tramadol glucuronide in human urine using capillary electrophoresis with laser-induced native fluorescence detection. *J Chromatogr B Biomed Sci Appl*. 2001;765(1):3-13.
33. Rodgers T, Rowland M. Physiologically based pharmacokinetic modelling 2: predicting the tissue distribution of acids, very weak bases, neutrals and zwitterions. *J Pharm Sci*. 2006;95(6):1238-1257.
34. T'Jollyn H, Snoeys J, Colin P, et al. Physiology-based IVIVE predictions of tramadol from in vitro metabolism data. *Pharm Res*. 2015;32(1):260-274.
35. Food and Drug Administration. ULTRAM® (tramadol hydrochloride) tablets [prescribing information]. https://www.accessdata.fda.gov/drugsatfda_docs/label/2009/020281s032s033lbl.pdf. Accessed December 1, 2019.
36. Poulsen L, Arendt-Nielsen L, Brosen K, Sindrup SH. The hypoalgesic effect of tramadol in relation to CYP2D6. *Clin Pharmacol Ther*. 1996;60(6):636-644.
37. Schmitt W. General approach for the calculation of tissue to plasma partition coefficients. *Toxicol In Vitro*. 2008;22(2):457-467.
38. Ardakani YH, Rouini MR. Pharmacokinetic study of tramadol and its three metabolites in plasma, saliva and urine. *DARU J Pharm Sci*. 2009;14(4):245-255.
39. Zhou X, Liu J. Fluorescence detection of tramadol in healthy Chinese volunteers by high-performance liquid chromatography and bioequivalence assessment. *Drug Des Devel Ther*. 2015;9:1225-1231.
40. Ochs HR, Greenblatt DJ, Woo E, Smith TW. Reduced quinidine clearance in elderly persons. *Am J Cardiol*. 1978;42(3):481-485.
41. Ochs HR, Greenblatt DJ, Woo E. Clinical pharmacokinetics of quinidine. *Clin Pharmacokinet*. 1980;5(2):150-168.
42. Hamelin BA, Bouayad A, Methot J, et al. Significant interaction between the nonprescription antihistamine diphenhydramine and the CYP2D6 substrate metoprolol in healthy men with high or low CYP2D6 activity. *Clin Pharmacol Ther*. 2000;67(5):466-477.
43. Regardh CG, Johnsson G. Clinical pharmacokinetics of metoprolol. *Clin Pharmacokinet*. 1980;5(6):557-569.
44. Nielsen TL, Rasmussen BB, Flinois JP, Beaune P, Brosen K. In vitro metabolism of quinidine: the (3S)-3-hydroxylation of quinidine is a specific marker reaction for cytochrome P-4503A4 activity in human liver microsomes. *J Pharmacol Exp Ther*. 1999;289(1):31-37.
45. Madani S, Paine MF, Lewis L, Thummel KE, Shen DD. Comparison of CYP2D6 content and metoprolol oxidation between microsomes isolated from human livers and small intestines. *Pharm Res*. 1999;16(8):1199-1205.
46. Ching MS, Blake CL, Ghabrial H, et al. Potent inhibition of yeast-expressed CYP2D6 by dihydroquinidine, quinidine, and its metabolites. *Biochem Pharmacol*. 1995;50(6):833-837.
47. VandenBrink BM, Foti RS, Rock DA, Wienkers LC, Wahlstrom JL. Prediction of CYP2D6 drug interactions from in vitro data: evidence for substrate-dependent inhibition. *Drug Metab Dispos*. 2012;40(1):47-53.
48. Ochs HR, Greenblatt DJ, Woo E, Franke K, Pfeifer HJ, Smith TW. Single and multiple dose pharmacokinetics of oral quinidine sulfate and gluconate. *Am J Cardiol*. 1978;41(4):770-777.
49. Guentert TW, Holford NH, Coates PE, Upton RA, Riegelman S. Quinidine pharmacokinetics in man: choice of a disposition model and absolute bioavailability studies. *J Pharmacokinet Biopharm*. 1979;7(4):315-330.
50. Kirchheiner J, Heesch C, Bauer S, et al. Impact of the ultrarapid metabolizer genotype of cytochrome P450 2D6 on metoprolol pharmacokinetics and pharmacodynamics. *Clin Pharmacol Ther*. 2004;76(4):302-312.
51. Clinical drug interaction studies — Cytochrome P450 enzyme- and transporter-mediated drug interactions. FDA Guidance for Industry; 2020.
52. Campanero MA, Calahorra B, Valle M, Troconiz IF, Honorato J. Enantiomeric separation of tramadol and its active metabolite in human plasma by chiral high-performance liquid chromatography: application to pharmacokinetic studies. *Chirality*. 1999;11(4):272-279.
53. T'Jollyn H, Snoeys J, Vermeulen A, et al. Physiologically based pharmacokinetic predictions of tramadol exposure throughout pediatric life: an analysis of the different clearance contributors with emphasis on CYP2D6 maturation. *AAPS J*. 2015;17(6):1376-1387.
54. T'Jollyn H, Snoeys J, Van Bocxlaer J, et al. Strategies for determining correct cytochrome P450 contributions in hepatic clearance predictions: in vitro-in vivo extrapolation as modelling approach and tramadol as proof-of-concept compound. *Eur J Drug Metab Pharmacokinet*. 2017;42(3):537-543.
55. T'Jollyn H, Vermeulen A, Van Bocxlaer J. PBPK and its virtual populations: the impact of physiology on pediatric pharmacokinetic predictions of tramadol. *AAPS J*. 2018;21(1):8.
56. Xu M, Zheng L, Zeng J, Xu W, Jiang X, Wang L. Physiologically based pharmacokinetic modeling of tramadol to inform dose adjustment and drug-drug interactions according to CYP2D6 phenotypes. *Pharmacotherapy*. 2021;41(3):277.
57. Metoprolol succinate extended-release tablets, NDA 19-962, S-032. https://www.accessdata.fda.gov/drugsatfda_docs/label/2006/019962s032lbl.pdf. Accessed November 1, 2020.
58. Matic M, de Wildt SN, Elens L, et al. SLC22A1/OCT1 Genotype affects O-desmethyltramadol exposure in newborn infants. *Ther Drug Monit*. 2016;38(4):487-492.
59. Stamer UM, Musshoff F, Stuber F, Brockmoller J, Steffens M, Tzvetkov MV. Loss-of-function polymorphisms in the organic cation transporter OCT1 are associated with reduced postoperative tramadol consumption. *Pain*. 2016;157(11):2467-2475.
60. Sheikholeslami B, Gholami M, Lavasani H, Rouini M. Evaluation of the route dependency of the pharmacokinetics and neuro-pharmacokinetics of tramadol and its main metabolites in rats. *Eur J Pharm Sci*. 2016;92:55-63.
61. Kitamura A, Higuchi K, Okura T, Deguchi Y. Transport characteristics of tramadol in the blood-brain barrier. *J Pharm Sci*. 2014;103(10):3335-3341.
62. McAinsh J, Cruickshank JM. Beta-blockers and central nervous system side effects. *Pharmacol Ther*. 1990;46(2):163-197.
63. Kusuhara H, Suzuki H, Terasaki T, Kakee A, Lemaire M, Sugiyama Y. P-glycoprotein mediates the efflux of quinidine across the blood-brain barrier. *J Pharmacol Exp Ther*. 1997;283(2):574-580.

64. Fonne-Pfister R, Bargetzi MJ, Meyer UA. MPTP, the neurotoxin inducing Parkinson's disease, is a potent competitive inhibitor of human and rat cytochrome P450 isozymes (P450bufI, P450db1) catalyzing debrisoquine 4-hydroxylation. *Biochem Biophys Res Commun*. 1987;148(3):1144-1150.
65. Allegaert K, van den Anker JN, de Hoon JN, et al. Covariates of tramadol disposition in the first months of life. *Br J Anaesth*. 2008;100(4):525-532.

Supplemental Information

Additional supplemental information can be found by clicking the Supplements link in the PDF toolbar or the Supplemental Information section at the end of web-based version of this article.